

A SEMI-ANALYTICAL APPROACH TO SIX-DIMENSIONAL PATH-DEPENDENT TRANSPORT MATRICES WITH APPLICATION TO HIGH-BRIGHTNESS CHARGED-PARTICLE BEAM TRANSPORT*

C.-Y. Tsai[†], K. Fan, Huazhong University of Science and Technology, Wuhan, China

Abstract

Efficient and accurate estimate of high-brightness electron beam dynamics is an important step to the overall performance evaluation in modern particle accelerators. Utilizing the moment description to study multi-particle beam dynamics, it is necessary to develop a path-dependent transport matrix, together with application of the drift-kick algorithm. In this paper we will construct semi-analytical models for two typical beam transport elements, solenoid with fringe fields and transverse deflecting cavity. To construct the semi-analytical models for these elements, we begin by formulating the simplified single-particle equations of motion, and apply numerical techniques to solve the corresponding six-by-six transport matrix as a function of the path coordinate. The developed semi-analytical models are demonstrated with practical examples, where the numerical results are discussed, compared with and validated by particle tracking simulations. These path-dependent transport matrix models can be incorporated to the analysis based on beam matrix method for the application to high-brightness charged-particle beam transport.

SEMI-ANALYTICAL MODELS

We note that the mathematical notations follow [1].

Solenoid with Fringe Field

Assuming the longitudinal magnetic field B_s is collinear with z , to first order in the spatial (circular cylindrical) coordinate, we have the radial and azimuthal magnetic field components $B_r \approx -\frac{r}{2}B'_s$ and $B_\phi = 0$, respectively. Here r is the radial distance from the solenoid axis. Written in Cartesian coordinate, we have $\mathbf{B} = \left(-\frac{1}{2}B'_s x, -\frac{1}{2}B'_s y, B_s\right)$. Neglecting the longitudinal effect of the solenoid, which is of the second order [2], we can write down the single-particle equations of motion in the transverse phase space coordinate $\mathbf{X}_{4D} = (x, x', y, y')$ as [2]

$$x'' = \mathcal{S}(s)y' + \frac{1}{2}\mathcal{S}'(s)y, \quad (1a)$$

$$y'' = -\mathcal{S}(s)x' - \frac{1}{2}\mathcal{S}'(s)x, \quad (1b)$$

where $\mathcal{S}(s) = eB_s(s)/\gamma m\beta c = B_s(s)/[B\rho]$ with $[B\rho]$ the beam rigidity. The formula $[B\rho]$ (T-m) = $3.3356 \times \beta E$ (GeV) can be of practical use.

Here we recommend that the interested reader to [3] for a more detailed discussion of single-particle dynamics in

* The work was supported by the Fundamental Research Funds for the Central Universities under Project No. 5003131049.

[†] jcytsai@hust.edu.cn

a solenoid magnetic field. For convenience of the subsequent analysis, we perform a coordinate rotation in complex notation and define $\eta_L = x_L + iy_L$, with the subscript L denoting a (complex) quantity in Larmor frame. The solution to Eq. (1) can be generally expressed as

$$\begin{bmatrix} \eta_L \\ \eta'_L \end{bmatrix}_s = \begin{pmatrix} M_{L,11} & M_{L,12} \\ M_{L,21} & M_{L,22} \end{pmatrix} \begin{bmatrix} \eta_L \\ \eta'_L \end{bmatrix}_{s_i}. \quad (2)$$

Note that $M_{L,ij}$ is also a complex quantity in Larmor frame. The evolution equations for $M_{L,ij}$ can be written as [2]

$$\frac{dM_{L,11}}{ds} = M_{L,21}, \quad \frac{dM_{L,12}}{ds} = M_{L,22}, \quad (3a)$$

$$\frac{dM_{L,21}}{ds} = -\frac{i}{2}\mathcal{S}'(s)M_{L,11} - i\mathcal{S}(s)M_{L,21}, \quad (3b)$$

$$\frac{dM_{L,22}}{ds} = -\frac{i}{2}\mathcal{S}'(s)M_{L,12} - i\mathcal{S}(s)M_{L,22}. \quad (3c)$$

Now we convert η_L to x_L and y_L by taking the real and imaginary parts, respectively. The 2×2 matrix in Eq. (2) now becomes 4×4 with

$$\begin{bmatrix} x_L \\ x'_L \\ y_L \\ y'_L \end{bmatrix}_s = \begin{pmatrix} M_{L,11}^{\text{Re}} & M_{L,12}^{\text{Re}} & -M_{L,11}^{\text{Im}} & -M_{L,12}^{\text{Im}} \\ M_{L,21}^{\text{Re}} & M_{L,22}^{\text{Re}} & -M_{L,21}^{\text{Im}} & -M_{L,22}^{\text{Im}} \\ M_{L,11}^{\text{Im}} & M_{L,12}^{\text{Im}} & M_{L,11}^{\text{Re}} & M_{L,12}^{\text{Re}} \\ M_{L,21}^{\text{Im}} & M_{L,22}^{\text{Im}} & M_{L,21}^{\text{Re}} & M_{L,22}^{\text{Re}} \end{pmatrix} \begin{bmatrix} x_L \\ x'_L \\ y_L \\ y'_L \end{bmatrix}_{s_i}, \quad (4)$$

where the superscripts Re and Im denote the real and imaginary part of a matrix element, respectively. As a final step, we transform the quantities from Larmor frame back to the Lab frame by \mathbf{R}^{-1} (Lab \rightarrow Larmor), where \mathbf{R} (Lab \rightarrow Larmor) =

$$\begin{pmatrix} \cos \Delta\theta_L & 0 & \sin \Delta\theta_L & 0 \\ -\Delta\theta'_L \sin \Delta\theta_L & \cos \Delta\theta_L & \Delta\theta'_L \cos \Delta\theta_L & \sin \Delta\theta_L \\ -\sin \Delta\theta_L & 0 & \cos \Delta\theta_L & 0 \\ -\Delta\theta'_L \cos \Delta\theta_L & -\sin \Delta\theta_L & -\Delta\theta'_L \sin \Delta\theta_L & \cos \Delta\theta_L \end{pmatrix}, \quad (5)$$

with Larmor angle defined as $\Delta\theta_L = -\frac{1}{2} \int_{s_0}^s \mathcal{S}(\zeta) d\zeta$. Here positive B_s gives positive Larmor angle (i.e., $e < 0$).

From the above analysis, given the longitudinal magnetic field profile B_s , we can numerically solve Eq. (3) [by using a standard finite difference scheme, for example] to obtain $M_L(s)$. Multiplying the inverse matrix of Eq. (5) with the obtained $M_L(s)$ and appending the longitudinal block matrix as a drift section of the length ranging from $s = 0$ to $s = L_{\text{sol}}$ thus gives the 6×6 transport matrix $\mathbf{M}_{\text{sol}}(s)$ for the solenoid. The resulting transport matrix is s -dependent and includes

the effect of fringe fields. Here we comment that, as for construction of the solenoid transport matrix with fringe fields, Migliorati and Dattoli [4] proceeds with analytical analysis of Eq. (3) by introducing the umbral variable and gave an exact solution to Eq. (3) as a function of s .

Transverse Deflecting Structure (TDS)

Let us consider a circular-cylindrical cavity with TM_{110} mode. The explicit field expressions can be analytically obtained [5, 6]. Under paraxial approximation the fields inside TDS can be approximately expressed as $B_y = B_0 \cos(\omega t + \phi_0)$ and $E_z = -B_0 \omega x \sin(\omega t + \phi_0)$ (ϕ_0 is the initial phase seen by the passing electron at the entrance of TDS). Given the simplified field expressions, we may construct the single-particle equations of motion based on Lorentz force equation. Let us write the 6-D phase space coordinate as $\mathbf{X} = (\mathbf{r}, \mathbf{p})$. Then we have $d\mathbf{p}/dt = \mathbf{F} = -e(\mathbf{E} + c\boldsymbol{\beta} \times \mathbf{B})$ and $d\mathbf{r}/dt = \mathbf{p}/\gamma m$, $\gamma = 1/\sqrt{1-\beta^2}$, $\beta = v/c$. The equations of motion can be explicitly written as

$$\frac{dp_x}{dt} = ev_z B_0 \cos(\omega t + \phi_0), \quad \frac{dp_y}{dt} = 0, \quad (6a)$$

$$\frac{dp_z}{dt} = eB_0 \omega x \sin(\omega t + \phi_0) + ev_x B_0 \cos(\omega t + \phi_0), \quad (6b)$$

$$\frac{dx}{dt} = \frac{p_x}{\gamma m}, \quad \frac{dy}{dt} = \frac{p_y}{\gamma m}, \quad \frac{dz}{dt} = \frac{p_z}{\gamma m}. \quad (6c)$$

Having obtained the single-particle equations of motion, we will track a few representative particles at each location s , and then extract the total of 36 transport matrix elements (at each s). We will illustrate the numerical procedures below. For simplicity, we only consider the 4-D (x, x', z, z') case. It is straightforward to extend to 6-D case by including (y, y') . Assume we have sixteen independent representative particles, of which the individual 4-D phase space coordinate denotes $\mathbf{X}_{4D}^{(i)} = (x^{(i)}, x'^{(i)}, z^{(i)}, z'^{(i)})$, where $i = 1 \sim 16$. Our goal is to find the sixteen transport matrix elements corresponding to Eq. (6). For a total of sixteen representative particles, the full set of linear transport equations can be written as $\mathbf{Z}_{16 \times 16}^i \mathbf{R}_{16 \times 1}^{i \rightarrow f}(s) = \mathbf{Z}_{16 \times 1}^f(s)$, where $\mathbf{Z}_{16 \times 16}^i$ contains four block diagonal matrices with

$$\mathbf{Z}_{16 \times 16}^i = \begin{pmatrix} \mathcal{Z}_{4 \times 4}^{(1-4)} & 0 & 0 & 0 \\ 0 & \mathcal{Z}_{4 \times 4}^{(5-8)} & 0 & 0 \\ 0 & 0 & \mathcal{Z}_{4 \times 4}^{(9-12)} & 0 \\ 0 & 0 & 0 & \mathcal{Z}_{4 \times 4}^{(13-16)} \end{pmatrix}, \quad (7)$$

$$\text{with } \mathcal{Z}_{4 \times 4}^{(1-4)} = \begin{bmatrix} \mathbf{X}_{4D}^{(1)} & \mathbf{X}_{4D}^{(2)} & \mathbf{X}_{4D}^{(3)} & \mathbf{X}_{4D}^{(4)} \end{bmatrix}^T.$$

Since $\mathbf{Z}_{16 \times 1}^i$ is given and $\mathbf{R}_{16 \times 1}^{i \rightarrow f}(s)$ are already obtained by numerically integrating Eqs. (6), we can find $\mathbf{R}_{16 \times 1}^{i \rightarrow f}(s)$ at each s by inverting $\mathbf{Z}_{16 \times 16}^i$. The standard form of 6×6 transport matrix (at each s) can be obtained by reshaping $\mathbf{R}_{16 \times 1}^{i \rightarrow f}(s)$. Here we note that an excellent and thorough discussion of beam dynamics in a TDS and its practical cavity cell design can be found in [7] using particle tracking simulation ASTRA [8].

NUMERICAL COMPARISONS

Solenoid with Fringe Field

For the case of a solenoid with fringe field, a longitudinal magnetic field profile B_s along s is constructed as follows

$$B_s(s) = B_{z0} \frac{\text{erf}\left(\frac{s-L_{\text{sol}}/4}{\kappa}\right) - \text{erf}\left(\frac{s-3L_{\text{sol}}/4}{\kappa}\right)}{2\text{erf}\left(\frac{L_{\text{sol}}}{2\kappa}\right)}, \quad (8)$$

where B_{z0} is the uniform flattop field amplitude, L_{sol} is the total length of the solenoid, and κ is characteristic of the (symmetric) fall-off fringe fields. In Eq. (8), the smaller the κ is, the sharper the edge field will be. In the following numerical example, we choose $\kappa = 0.01$.

Given $B_s(s)$, $\mathcal{S}(s)$ can be obtained. According to Eq. (3), the 4×4 transport matrix in Larmor frame can be numerically integrated. Transforming back to the Lab frame by Eq. (5) and appending the longitudinal block matrix as a drift section give the 6×6 solenoid transport matrix as a function of s . In the following numerical setup, the uniform flattop B_{z0} is assumed 0.05 T, the total length of the solenoid $L_{\text{sol}} = 0.1$ m, and the beam energy is set 3 MeV. Having obtained the 6×6 single-particle transport matrix for the solenoid as a function of s , we can evaluate the multi-particle beam dynamics by propagating the beam sigma matrix according to the method outlined in [1], illustrated in Fig. 1. In the figure we also compare our semi-analytical calculation with particle tracking simulations by ASTRA [8] and obtain a good agreement.

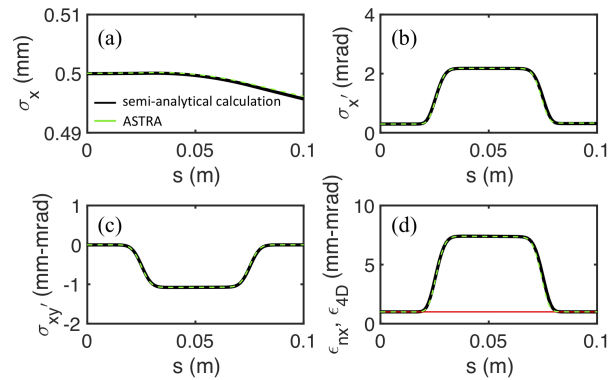


Figure 1: (a) Transverse rms beam size as a function of s ; (b) transverse rms beam divergence as a function of s ; (c) transverse $x - x'$ correlation as a function of s ; (d) transverse emittances as a function of s . The red line in (d) refers to the transverse 4-D emittance, which is conserved along s .

Having obtained the solenoid transport matrix and the evolution of beam properties along s , we may vary the solenoid field amplitude B_{z0} to see the dependence of the transverse beam size and divergence at the exit. Figure 2 shows the results from our semi-analytical calculation with comparison of particle tracking simulation [8]. Comparison with particle tracking simulation (blue dots in Fig. 2) shows a good

Content from this work may be used under the terms of the CC BY 3.0 licence (© 2019). Any distribution of this work must maintain attribution to the author(s), title of the work, publisher, and DOI

agreement except for larger B_{z0} , where we think that the deviation may stem from the slightly different count of Larmor angle in our semi-analytical model from the more accurate calculation by ASTRA, in which the on-axis and off-axis particles will receive slightly different Larmor angles.

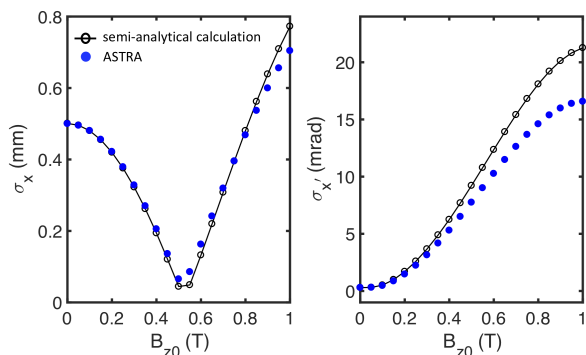


Figure 2: (Left) beam size and (right) beam divergence at the exit of the solenoid as a function of the field strength. In the numerical setup, for the solenoid $\kappa = 0.01$ m and $L_{sol} = 0.1$ m. The initial beam size is assumed 0.5 mm, with the normalized emittance $1 \mu\text{m}$.

Transverse Deflecting Structure (TDS)

According to Faraday's law, the corresponding TDS voltage can be evaluated by $V_{TDS} = cB_0L_{TDS}$, with L_{TDS} the length of the TDS. In the following numerical demonstration we will validate our semi-analytical model by the analytical formulas for the bulk of TDS [5] and by particle tracking simulation ELEGANT [9]. In the numerical setup, the deflecting magnetic field B_0 is assumed 0.05 T, which corresponds to $V_{TDS} = 0.75$ MV, the TM_{110} operating frequency is set 3 GHz, the initial phase $\phi_0 = 0$, the total length of the TDS $L_{TDS} = 0.05$ m, and the beam energy is still set 3 MeV.

Figure 3 draws typical beam characteristics as a function of the deflecting strength B_0 at the exit. Since the TDS introduces a transverse momentum to the beam, this momentum will lead to possible increase of beam size via $x - x'$ correlation M_{12} . Moreover this transverse momentum varies with time (or, z), which means that the transverse defocusing strength varies along z , and can eventually lead to growth of projected beam emittance.

It is found that our semi-analytical model appears to overestimate the transverse defocusing, while the results from ELEGANT tracking and analytical prediction give negligible increase of the transverse beam size. As previously discussed, the induced transverse momentum will result in possible growth of projected beam emittance, shown in Fig. 3(b), where both our semi-analytical calculation and ELEGANT tracking reveal this trend, while the prediction by analytical formulas [5] give a constant value over TDS deflecting strength. Because of the presence of the longitudinal electric field in the TDS, particles in the beam may

induce an additional energy spread, depending on the deflecting strength of TDS. The growth of energy spread is shown in Fig. 3(d), where our semi-analytical results are consistent (but overestimated) with that by particle tracking simulation. Again, the prediction by analytical formulas [5] gives a constant value over TDS deflecting strength. From the comparisons, we find that some beam characteristics, σ_z , is consistent among the three approaches; in the meanwhile other characteristics may be given with different results based on different methods. More detailed studies, including the underlying assumptions for different models between particle tracking and semi-analytical calculation, will be necessary to investigate the beam dynamics in the TDS.

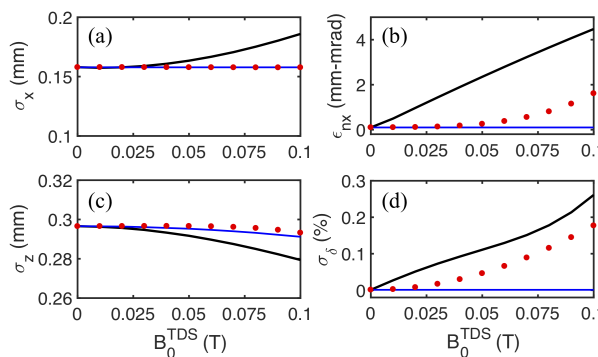


Figure 3: Dependence on the magnetic deflecting field for (a) beam size and; (b) beam emittance; (c) bunch length; (d) the relative energy spread, at the exit of the TDS. The black lines are obtained from our semi-analytical model, the blue lines from the analytical formulas by van Rens *et al.* [5], and the red dots from particle tracking simulation ELEGANT.

SUMMARY

In this paper we have constructed 6×6 s -dependent transport matrices for two practical transport elements, the solenoid with fringe fields and the TDS. In constructing the solenoid transport matrix, the fringe fields at the entrance and exit are taken into account. The results from our semi-analytical model are compared with ASTRA and a good agreement is shown. In constructing the TDS transport matrix, we track a few representative particles, find the inverse \mathbf{Z} matrix, and extract the transport matrix elements as a function of s . We have then compared the numerical results with the analytical formulas by van Rens *et al.* [5] at the TDS exit. We also compared our results with particle tracking simulation by ELEGANT and obtained a reasonable agreement. We comment that the developed TDS model does not take the edge fields into account, i.e., the hard edge model. We put emphasis on the developed semi-analytical models that they can be incorporated to our recent work [1] and will further enrich our tool for beam moment calculation.

REFERENCES

- [1] C.-Y. Tsai et al., “Low-energy high-brightness electron beam dynamics based on slice beam matrix method”, submitted for publication
- [2] H. Wiedemann, *Particle Accelerator Physics*. New York City, NY, USA: Springer, 2007.
- [3] V. Kumar, “Understanding the focusing of a charge particle beams in a solenoid magnetic field,” *Am. J. Phys.*, vol. 77, no. 8, p. 737-741, Jul. 2009. doi:10.1119/1.3129242
- [4] M. Migliorati and G. Dattoli, “Transport matrix of a solenoid with linear fringe field,” *Il Nuovo Cimento*, vol. 124, no. 4, pp. 385-394, Apr. 2009. doi:10.1393/ncb/i2009-10780-0
- [5] J.F.M. van Rens *et al.*, “Theory and particle tracking simulations of a resonant radiofrequency deflection cavity in TM110 mode for ultrafast electron microscopy,” *Ultramicroscopy*, vol. 184B, pp. 77-89, Jan. 2018. doi:10.1016/j.ultramic.2017.10.004
- [6] G. Stupakov and G. Penn, *Classical Mechanics and Electromagnetism in Accelerator Physics*. New York City, NY, USA: Springer, 2018.
- [7] K. Floettmann, “Beam dynamics in transverse deflecting rf structures,” *Phys. Rev. ST Accel. Beams* vol. 17, p. 024001, Feb. 2014. doi:10.1103/PhysRevSTAB.17.024001
- [8] A Space Charge Tracking Algorithm,
<http://www.desy.de/~mpyf10/>.
- [9] M. Borland, “elegant: A Flexible SDDS-Compliant Code for Accelerator Simulation,” presented at ICAP’00, Darmstadt, Germany, Sep. 2000.